DEVELOPMENT OF EC 135 TURBULENCE MODELS VIA SYSTEM IDENTIFICATION

S. Seher-Weiss and W. von Gruenhagen
DLR Institute of Flight Systems
Lilienthalplatz 7, 38108 Braunschweig, Germany
susanne.seher-weiss@dlr.de, wolfgang.gruenhagen@dlr.de

Abstract

The paper focuses on the development of empirical hover and low-speed turbulence models in particular for the EC 135 helicopter. The approach used is the Control Equivalent Turbulence Input method, i.e. the determination of control inputs required to generate aircraft angular and vertical rates in calm conditions that are consistent with rates observed when flying in atmospheric turbulence. For the extraction process, this method uses a mathematical model of the aircraft dynamics and aircraft angular and vertical rates measured during flight tests in turbulence. Analyzing and modeling the power spectral densities of the extracted control disturbances allows to generate low order equivalent turbulence models that can be used for control system optimization, handling qualities investigations, and pilot training. The paper describes the two applications of system identification within the development of the turbulence model: First a high fidelity state space model of the EC 135 helicopter model in hover has to be developed as a prerequisite for the extraction of the equivalent control input traces from flights tests in turbulence. Once the control equivalent turbulence input traces have been extracted and their power spectral densities determined, a second identification step yields the desired turbulence models. The paper also presents some validation of the derived turbulence models.

1. NOMENCLATURE

$A_{lon}, A_{lat}, A_{col}, A_{ped}$	turbulence filter amplitudes (longitudinal, lateral, collective, and pedal)
F	sampling frequency, Hz
j	imaginary unit
L_w, L_v	main rotor resp. tail rotor scaling parameter
S	power spectral density
s	Laplace variable
U_0	mean wind speed
W_{noise}	white noise input
w	window function (Hanning window)
ω	frequency, rad/s
$\delta_{lon}, \delta_{lat}, \delta_{col}, \delta_{ped}$	pilot control inputs (longitudinal, lateral, collective, and pedal)

2. INTRODUCTION

For helicopters, precision hover tasks in adverse weather conditions are an important mission but difficult to model in a real-time simulation. Reliable aircraft math models validated by flight test and hover turbulence models are needed.

The traditional approach to turbulence modeling for fixed wing aircraft is the use of a frozen gust pattern, most commonly generated from a Dryden spectral model. For frozen gust patterns, the reaction of the aircraft to the turbulence is a function of the relative velocity with respect to the air mass through which it is flying. Even though frozen gust patterns generated from Dryden turbulence models have received favorable comments at high speed forward flight, helicopter pilots have criticized them as not being representative for low speed flight [1]. Other approaches such as complex rotating frame turbulence models [2] are computationally expensive and thus not applicable in real-time. They can, however, be used for validation purposes.

Therefore, empirical hover and low speed turbulence models are being developed within the task “Modeling and Simulation for Rotorcraft Systems” of the US-German Memorandum of Understanding on Helicopter Aeromechanics. Here, the Control Equivalent Turbulence Input (CETI) approach is used to develop empirically based turbulence models. This method was first proposed by the National Research Council (NRC) Canada [3] and then extensively developed at the U.S. Army Aeroflightdynamics Directorate (AFDD) at Moffett Field California [4,5].

A CETI model of the UH-60 Black Hawk helicopter has successfully been developed from flight tests and validated [6]. The results showed good agreement between the CETI model and the more complex rotating-frame turbulence model SORBET (Simulation of Rotor Blade Element Turbulence).

DLR joined this activity to demonstrate the applicability of the CETI approach to a helicopter of different size (the size ratio of UH-60 to EC 135 is 10 to 2.8). The final aim of the turbulence modeling activities within the MOU is to arrive at a scalable model that is parameterized with helicopter specific parameters such as rotor diameter, rotor height, and tail rotor dimensions. The DLR results will enhance the database for developing such a scaling scheme.

FIG 1. The Flying Helicopter Simulator EC135 (FHS)

This paper presents an overview of the development of the CETI model for the EC 135 (FIG 1) with an emphasis on the use of system identification throughout the model development process.

3. CETI METHOD

The CETI method has been developed as an alternative means of accounting for turbulence during hovering and low-speed tasks, for which a turbulence model is most needed. It does not represent direct turbulence simulation in full aerodynamic details, but rather generates equivalent control inputs, which produce the same effect on the vehicle as turbulence itself. Due to the extraction from flight test data, the models are automatically validated for the specific helicopter type and therefore well suited for control system design when addressing disturbance rejection.

To generate such equivalent control inputs, data is collected from flights in different turbulence conditions and gusts. In order to keep the pilot inputs mostly uncorrelated from the turbulence itself, the pilot is instructed to just roughly hold the position without correcting all disturbances caused by turbulence. The measured aircraft responses are then usually fed into an inverse aircraft model to obtain control inputs related to pilot and gusts. Subtracting the measured pilot inputs yields equivalent control input traces that correspond to the response of the aircraft to the turbulence (see FIG 2 and [5]).

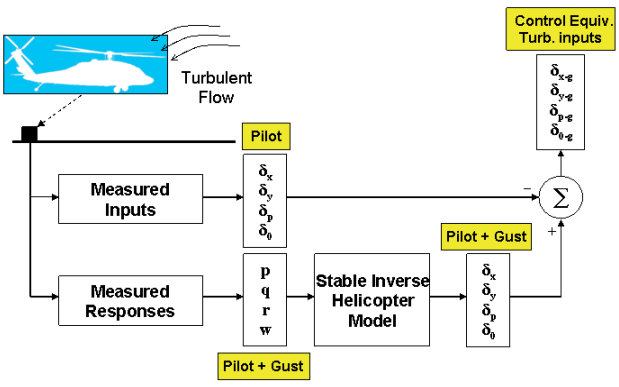

FIG 2. Gust extraction by inverse modeling

A different approach for extraction of the equivalent control inputs was proposed by Buchholz [7] (FIG 3). It does not need an inverse model of the aircraft, but instead an observer approach is used. The pilot inputs measured under turbulent conditions are fed into a nominal model of the aircraft to obtain the aircraft response caused by the pilot inputs. This calculated response is subtracted from the measured response (including gusts) and the error is minimized by feedback and added to the pilot inputs. The time histories of the feedback controls are then also related to the response of the aircraft due to the gusts. Compared to the first method, the observer approach, which is derived from control theory, provides a much simpler and elegant way of inverting the dynamic system.

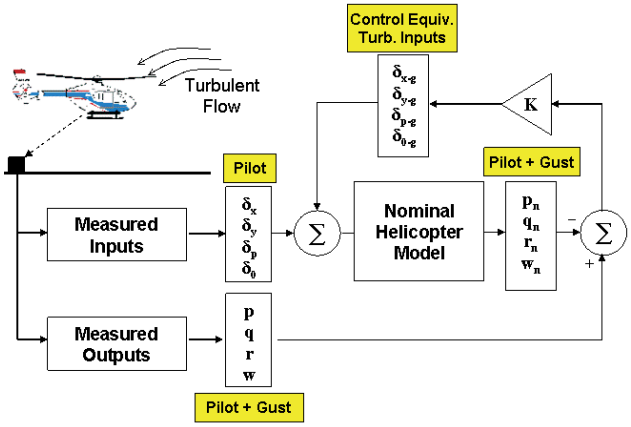

FIG 3. Gust extraction by observer

As the extracted control disturbances in both cases are used to develop white noise driven transfer functions of a form similar to Dryden models, their spectra have to be analyzed. Therefore, the power spectral densities (PSDs) of the control equivalent inputs for each control are first generated. These PSDs are then each approximated by a transfer function to capture the turbulence characteristics of the corresponding axis. This modeling process yields four transfer function filters, one for each control input. When using the CETI model for simulation, white noise is passed through these transfer function filters to generate control equivalent turbulence inputs which are then added to the pilot inputs.

4. MATH MODEL IDENTIFICATION

As the CETI extraction process is based on an error determination between flight tests with and without gusts, an accurate model of the helicopter dynamics must first be identified from flight tests without turbulence. The quasi-steady formulation of the helicopter dynamics by a classical 6-DoF rigid body model is valid only up to about 10 rad/s. To arrive at high fidelity models valid up to 30 rad/s, the higher order effects of rotor flapping, dynamic inflow, and rotor-lead-lag have to be accounted for.

For this identification task, the 6-DoF rigid body motion equations were first extended by modeling of the longitudinal and lateral flapping of the tip-path plane. As no blade measurements were available, an implicit model that incorporates roll and pitch acceleration as additional state variables was used instead of explicitly matching the flapping angles. The derivation of the corresponding model equations is given in [8].

To match the rising magnitude in the transfer function of vertical acceleration due to collective input at higher frequencies, modeling of the dynamic inflow was necessary. Again, an implicit model formulation with a 2nd order equation for the vertical velocity and the time derivative of the collective as input variable was used. The equations of this model that accounts for dynamic inflow but not for coning are derived in [8].

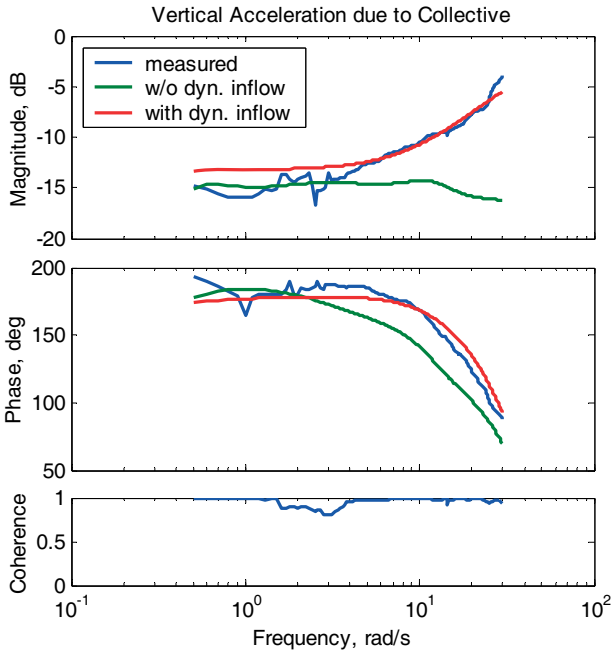

FIG 4. Frequency domain comparison for vertical acceleration due to collective Input

FIG 4 shows that modeling of the dynamic inflow is necessary to capture the amplitude increase in the frequency response for vertical acceleration due to collective input.

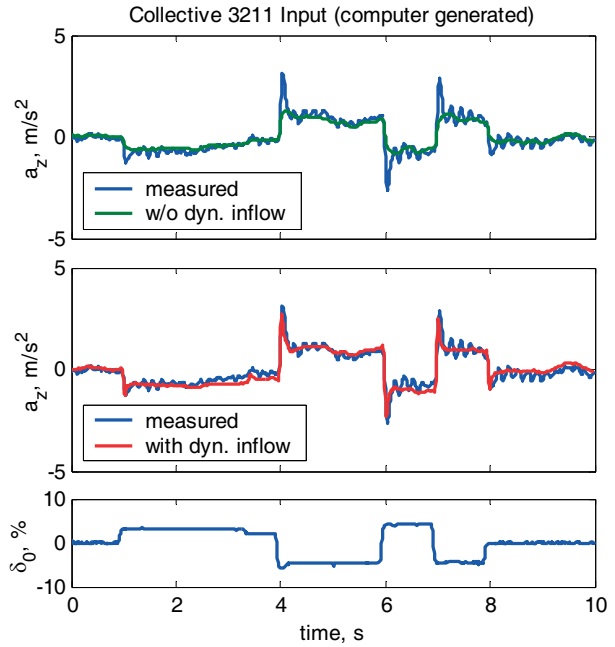

FIG 5. Time domain comparison for vertical acceleration due to collective input

FIG 5 compares the time responses of the identified models with and without dynamic inflow. It can clearly be seen that the model without dynamic inflow does not capture the initial overshoots in the vertical acceleration.

To model the responses in pitch and roll rates for frequencies up to 30 rad/s, the lead-lag effect has to also be accounted for. This was achieved by appending a second order dipole to the models for the pitch and roll rate responses due to longitudinal and lateral input as suggested in [9]. For implementation in a state-space identification model, the dipole transfer functions were transformed into state equations with instrumental variables as described in [8]. FIG 6 shows the improvement in the match of the on-axis transfer function in roll compared to the model without lead-lag. One can see, that for the EC 135 the lead-lag is a local effect around 12 rad/s.

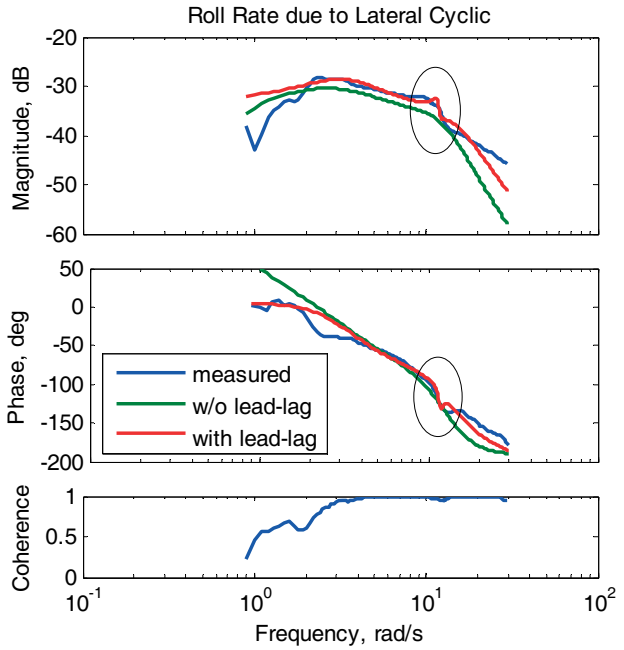

FIG 6. Transfer function comparison for roll due to lateral input

The above mentioned model improvements show, that the implicit modeling of rotor degrees of freedom, dynamic inflow, and lead-lag by embedding the classical equations into higher order equations, is a useful approach, when appropriate measurements are not available.

Using time and frequency domain methods, several models of varying complexity have been identified for the EC 135. They are currently used at DLR for different purposes:

- An 8-DoF model with flapping is used as a command model in the model following control system (MFCS).
- A 9-DoF model including flapping and dynamic inflow is used for the development of the feedback part of the MFCS.
- The identified dipole from the 11-DoF model was used for the design of a dipole compensator for the FHS [10,11].
- Both the 9-DoF and 11-DoF model have been used in the turbulence model development.

5. FLIGHT TESTS AND PSD ANALYSIS

5.1. Data Base

A first data gathering flight test was conducted in November 2007 on a day with relatively high turbulence where the tower recorded wind speeds of 23-34 kts. Seventeen different runs were conducted at two altitudes (20 ft and 40 ft AGL) and two different locations with respect to a line of trees (see FIG 7). It was expected that these trees would be generating additional ground vortices. Throughout all data gathering runs, the pilot was instructed to just roughly hold the position without correcting all disturbances caused by turbulence.

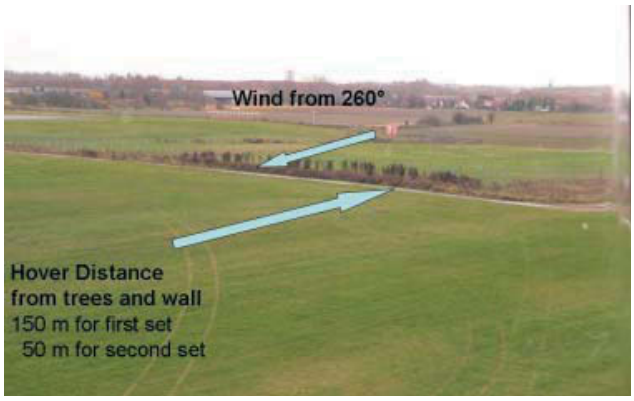

FIG 7. Test site for first turbulence data gathering flight

In December 2008 another data gathering flight was conducted. The aim of this second flight was to investigate whether the direction of the gusts with respect to the helicopter has any influence on the extracted CETIs. Thus, starting from the helicopter heading into the wind, the helicopter was rotated in 45° increments. This test was conducted at two different altitudes (30 ft and 90 ft AGL). During this second campaign, the turbulence was weaker with wind speeds of 15-18 kts.

5.2. Calculation of Power Spectral Densities

The CETI traces were extracted from all runs and the power spectral densities determined for each input. For this calculation the signals were windowed with overlapping Hanning windows and the autospectra determined using a chirp-z transform based routine.

$$(1) \quad S(e^{j\omega}) = \frac{\frac{1}{n}\left|\sum_{l=1}^{n} w_l x_l e^{j\omega l}\right|}{\frac{1}{n}\sum_{l=1}^{n}\left|w_l\right|^2}$$

The PSD was then calculated by taking the results for different window sizes and forming a weighted average, where the weighting function for each window length was taken from [12]. Throughout the figures in this paper, power spectral density scaled with sampling frequency (in Hz) is used.

$$(2) \quad PSD = S(e^{j\omega})/F$$

5.3. PSD Analysis

At the beginning of the analysis, the extraction process itself was validated. FIG 8 shows that the extraction by the observer approach is equivalent to the extraction by a stabilized inverse model of the helicopter. No discernible differences between the two extraction methods can be found in the region of interest of 0.5-10 rad/s.

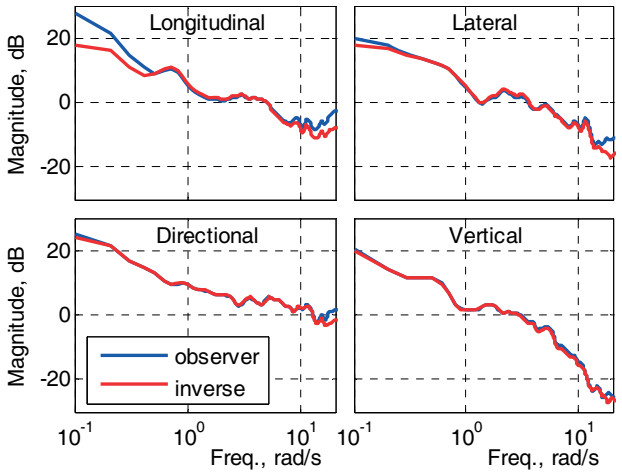

FIG 8. PSDs for CETIs from observer and inverse model

The comparison in FIG 9 shows that using the 11-DoF model (including lead-lag) yields nearly identical PSDs compared to using the 9-DoF model with only flapping and dynamic inflow. Differences can only be seen around the lead-lag frequency of 12 rad/s. As turbulence models shall be extracted by using a low order approximation, the lead-lag effect can be neglected and thus the 9-DoF model was used for the remainder of the investigations.

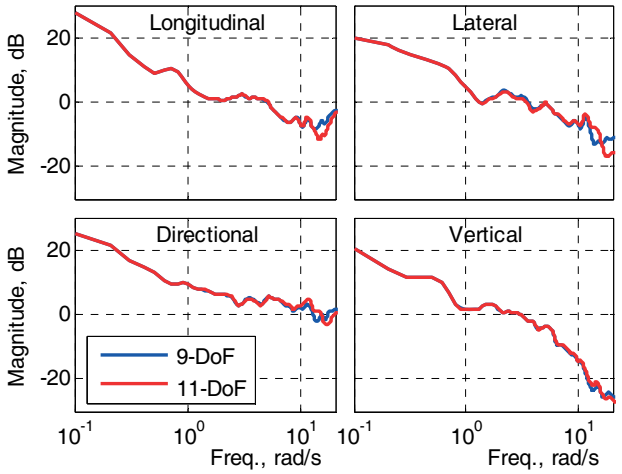

FIG 9. PSDs using 9-DoF and 11-DoF model

FIG 10 shows the coherence between the pilot inputs and the extracted CETI traces for all runs. It can be seen, that the coherence is quite low except for the lateral axis and low frequencies. This predominantly low coherence is attributed to the fact that the pilots were instructed to not directly correct the disturbances caused by the turbulence but to just roughly hold the position of the helicopter. As the helicopter is most agile in roll, more pilot control was needed in this axis to correct attitude excursions.

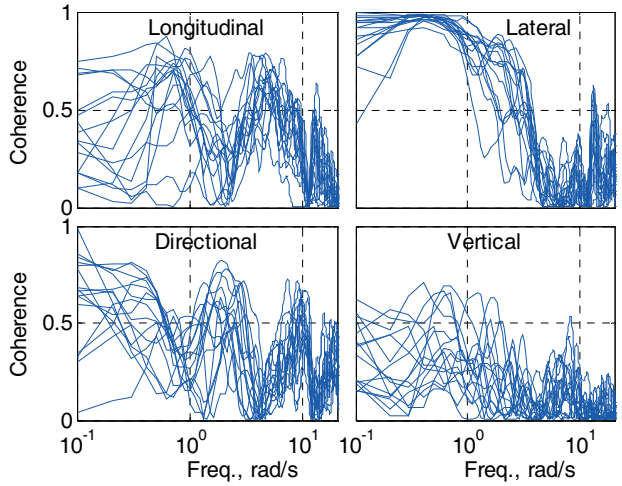

FIG 10. Coherence between pilot inputs and extracted CETIs

The local wind speed at the test location was recorded on ground during the first data gathering flight test using a handheld anemometer. FIG 11 shows the recorded wind speed over time in relation to the duration of the different flight test runs. It can be seen that the variation in wind speed, even within one run, was quite high.

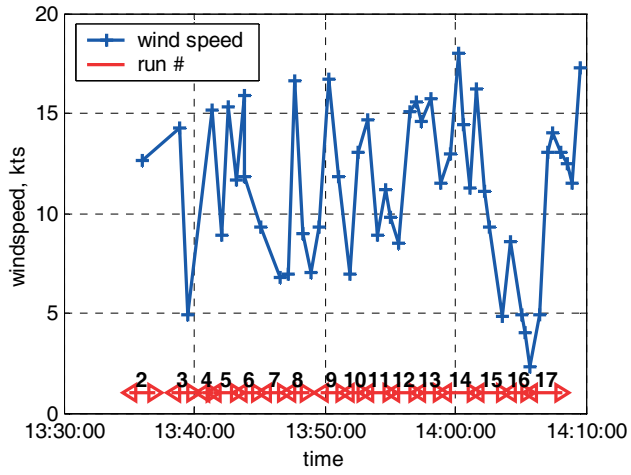

FIG 11. Recorded wind speed at the test location for the different runs

Run	Ground kts	Aircraft kts	Run	Ground kts	Aircraft kts
2	12.6	13.7 / 4.7	10	10.0	16.5 / 4.1
3	9.6	13.3 / 4.4	11	11.2	13.4 / 4.5
4	15.1	12.8 / 4.0	12	13.0	13.7 / 5.1
5	11.9	14.7 / 6.0	13	13.9	9.3 / 3.9
6	12.3	13.2 / 4.1	14	14.6	11.0 / 4.0
7	6.8	11.2 / 3.4	15	8.4	11.6 / 3.9
8	9.9	15.6 / 4.6	16	5.8	10.6 / 3.9
9	12.6	17.7 / 4.8	17	9.5	11.3 / 4.9

TAB 1. Wind speed measured on ground and on the aircraft

When grouping the runs of the first flight by test location (altitude and distance to the trees), no correlation between location and PSD level could be found. Furthermore, no dependency of PSD level on ground recorded airspeed was recognizable. Therefore, it was alternatively attempted to use the aircraft measured airspeed (calculated from aircraft static and dynamic pressure). Even though the absolute values of the aircraft measured airspeed are inaccurate below 30 kts, it should be possible to use them for grouping the runs.

TAB 1 compares the wind speed measured on the ground to the airspeed measured on the aircraft (mean and standard deviation for each run). The higher mean values of the aircraft measurements are due to the boundary layer profile above ground, i.e. the wind speed increases with height. FIG 12 shows that when grouping the runs by the onboard measured airspeed, an increase in turbulence level corresponds to increased levels of PSD in the extracted CETIs.

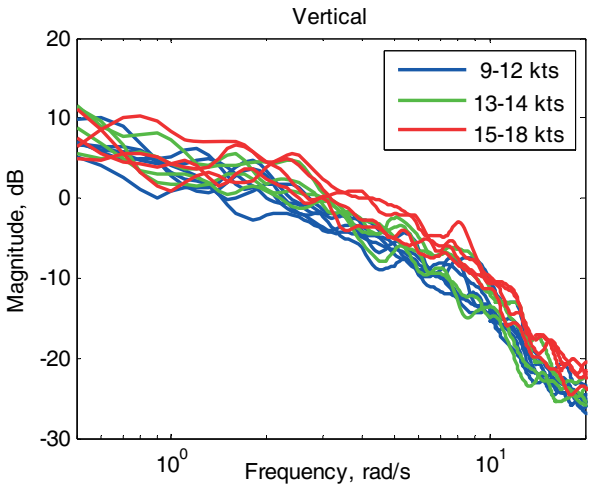

FIG 12. Extracted PSDs from runs with different mean wind speed (vertical axis)

FIG 13 shows the extracted power spectral densities from the runs at 90 ft AGL out of the second data gathering flight. No discernible differences between the different wind directions can be seen. The same holds for the runs at 30 ft AGL. This confirms the underlying assumption that the reaction to turbulence is solely a rotor effect. The same lack of dependency on wind direction had also been noted during earlier flight tests at DLR with the Bo 105 helicopter.

In summary, when analyzing the data from the two data gathering flights, the following conclusions could be drawn:

- Neither the test location (high/low and distance to trees) nor the wind direction has any influence on the extracted PSDs.
- The wind speed recorded on the ground during the tests is not usable for grouping the runs.
- Even though its absolute value is unreliable below 30 kts, the a/c recorded wind speed (mean value and standard deviation) can be used for grouping the runs into turbulence levels.

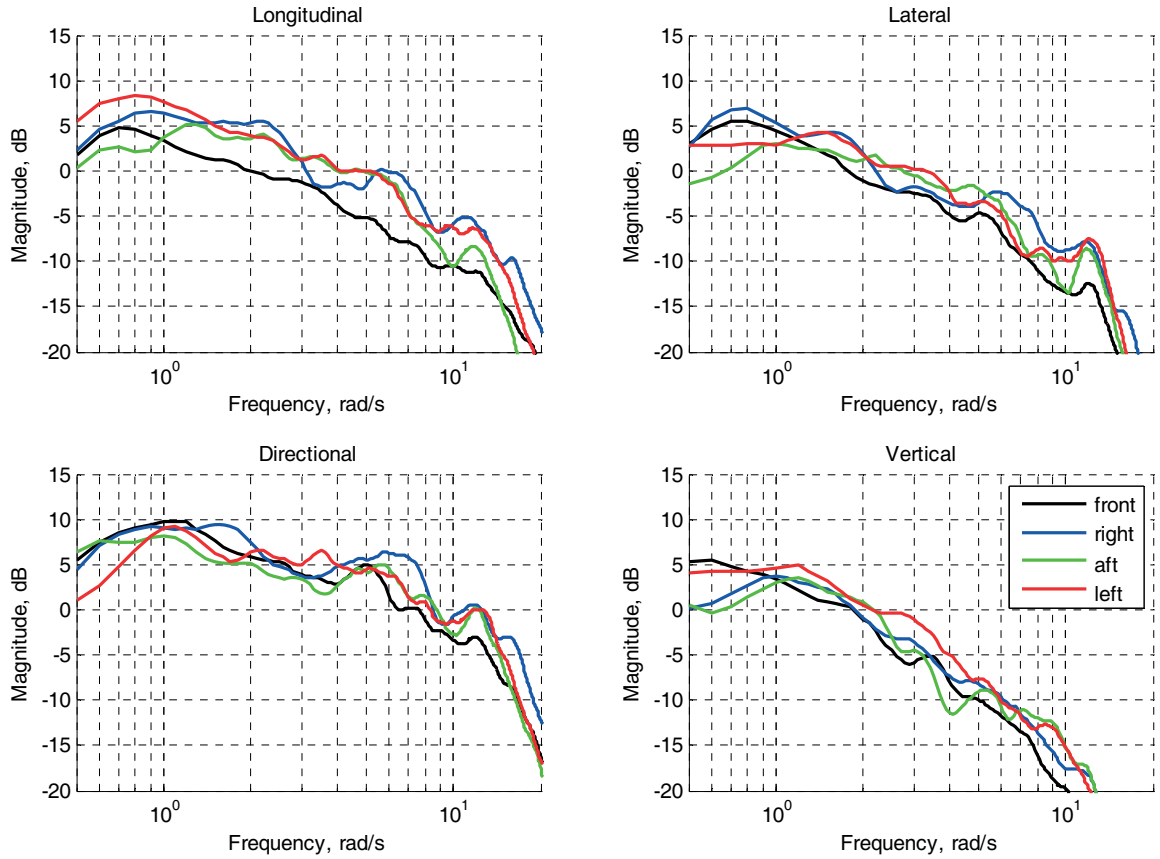

FIG 13. Extracted PSDs for wind from different directions

6. TURBULENCE MODEL IDENTIFICATION

6.1. Data Selection and Preprocessing

The aim of the modeling process was to develop turbulence models for different levels of turbulence. Regarding the data available from the two data gathering flights, three turbulence levels were chosen (see TAB 2). As the turbulence during the first flight was quite high, those runs from this flight with the lowest and highest wind speed were selected as medium resp. high turbulence, whereas runs from the second flight were used for low turbulence. For comparison, average wind speeds were also determined from flights for PID purposes that were presumably flown in conditions without turbulence.

Turbulence Level	Wind, mean, kts	Wind, StdDev., kts	Flight: runs
None	7.6	2.8	(PID flights)
Low	8.7	3.3	**2:** 8, 9, 10, 15
Medium	11.1	3.9	**1:** 4, 7, 13-15
High	15.4	5.1	**1:** 5, 8, 9, 12

TAB 2. Selected turbulence levels

The turbulence models shall be approximated for a frequency range of 0.5-10 rad/s. Therefore the extracted control equivalent turbulence inputs were band-pass filtered in the range 0.5-15 rad/s. From this filtered CETI data for the runs selected according to TAB 2, the PSDs were extracted and averaged over each turbulence level. The results in FIG 14 clearly show the three distinct turbulence levels.

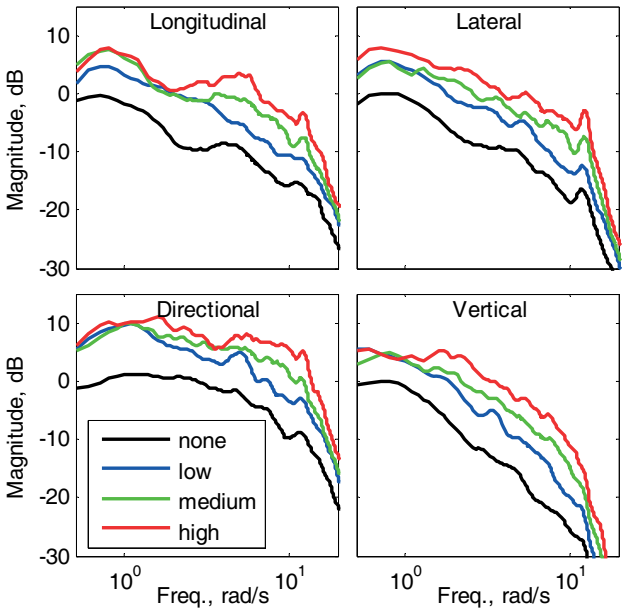

FIG 14. PSDs from filtered data for different turbulence levels

6.2. Model Extraction

Investigations have been conducted to determine estimates for the filter functions from physical and flow field considerations. According to [13], the turbulence models should have the following structure:

$$\text{(3a)}\quad \frac{\delta_{lon,gust}}{W_{noise}} = A_{lon}\frac{1}{(s+\frac{U_0}{L_w})}$$

$$\text{(3b)}\quad \frac{\delta_{lat,gust}}{W_{noise}} = A_{lat}\frac{1}{(s+\frac{U_0}{L_w})}$$

$$\text{(3c)}\quad \frac{\delta_{ped,gust}}{W_{noise}} = A_{ped}\frac{1}{(s+\frac{U_0}{L_v})}$$

$$\text{(3d)}\quad \frac{\delta_{col,gust}}{W_{noise}} = A_{col}\frac{(s+20\frac{U_0}{L_w})}{(s+0.63\frac{U_0}{L_w})(s+5\frac{U_0}{L_w})}$$

In order to confirm with this model structure, all turbulence model identification was don by performing a partially constraint fit using the transfer function approximation capabilities of FITLAB [14].

The approach for matching all four transfer function was as follows:

1. Match the longitudinal and lateral transfer functions with a common denominator.
2. Model the vertical transfer function with its poles and zeros restricted according to the model structure and the results from step 1.
3. Match the directional transfer function separately.

The results for all three turbulence levels are listed in TAB 3. One can see that there is a clear trend for each parameter with respect to turbulence level. The corresponding match between the extracted PSDs and the models can be seen in FIG 15.

Parameter	Low	Medium	High
A_{lon}	2.71	4.20	5.99
A_{lat}	2.56	3.92	6.07
U_0/L_w	1.57	2.31	3.00
A_{col}	0.473	0.676	0.974
A_{ped}	7.59	13.0	21.5
U_0/L_v	2.85	4.82	7.28

TAB 3. Identified turbulence model parameters

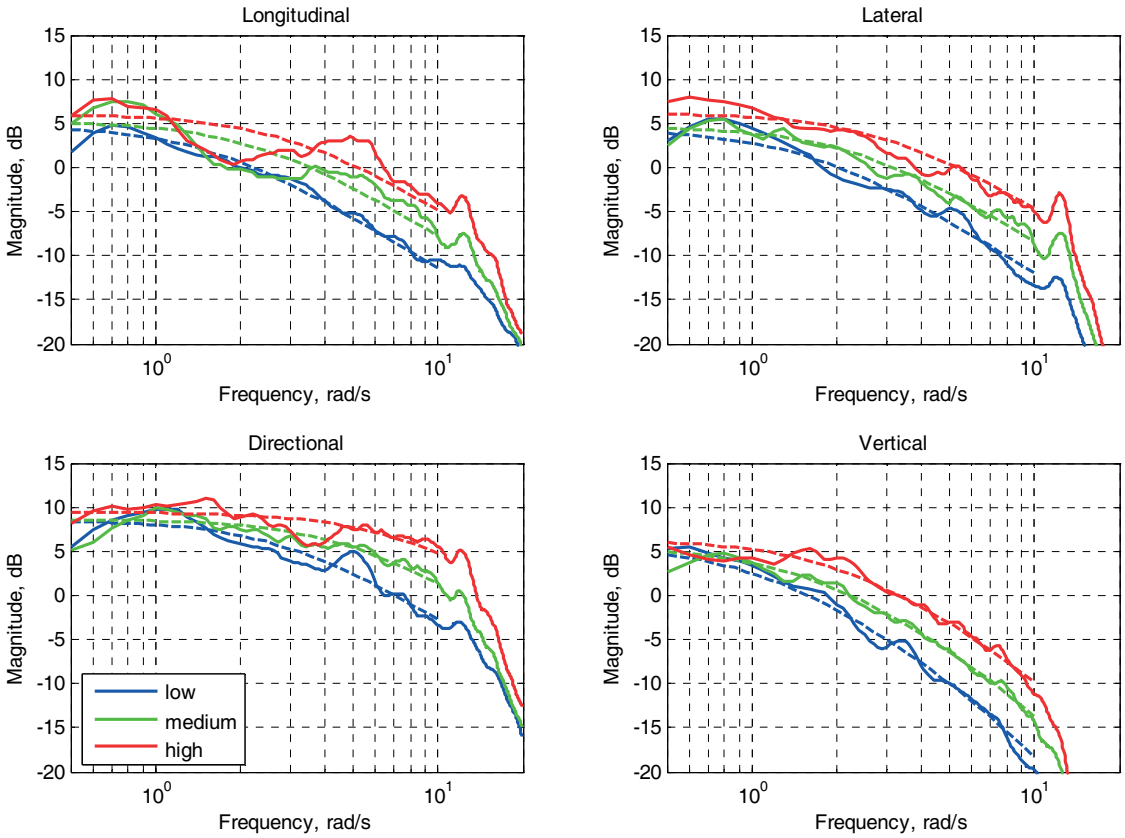

FIG 15. Match between extracted PSDs and identified models (solid line = PSD, dashed line = model)

7. TURBULENCE MODEL VALIDATION

7.1. Implementation

In a final step the identified turbulence models were used to simulate and validate the overall approach on the EC 135 Flying Helicopter Simulator (FHS) operated by DLR. The generated control inputs were fed into the mixer unit of the flight control system to simulate a flight in turbulence although flying in real calm air environment (see FIG 16). The turbulence generator was implemented using MATLAB/Simulink and Real-time-Workshop.

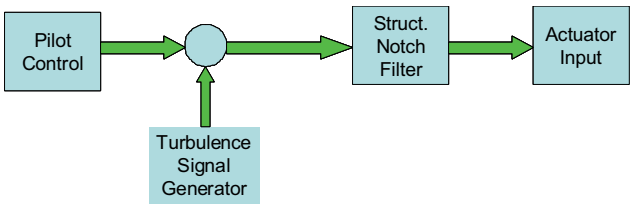

FIG 16. Implementation of turbulence generator on FHS

To check the implementation of the turbulence generator, the power spectral densities of the in-flight simulated CETIs were extracted as described above and the resulting PSDs compared to the underlying models. FIG 17 shows the results for 65 s length of data with a sampling interval of 0.008 s. It can be seen that the match is good, even though some fluctuation around the model still exists.

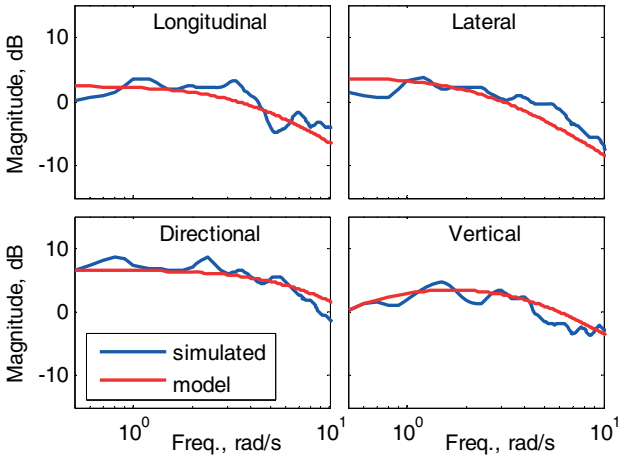

FIG 17. Comparison of PSDs between model and simulated CETIs

7.2. Simulated versus Extracted

Several flight tests were conducted where computer generated CETIs were added to the pilot inputs in all four control axes. The first test flight used some preliminary CETI models whereas the subsequent flights had refined models. For safety purposes, the added CETIs were scaled by an amplification factor that was incrementally set to 0.2, 0.5, and 0.8. Again, the same approach as above was used to extract CETIs and compare them to the generated CETIs and the underlying models.

FIG 18 shows the comparison between the PSDs of the simulated and extracted CETIs for a run with the preliminary model and an amplification factor of 0.8. It can be seen, that the PSDs of the extracted CETIs are a bit higher than what was simulated. The reason for this discrepancy is the fact, that the flight test was not conducted in calm air but in some weak basic turbulence. This is shown in FIG 18, where the PSDs of the basic turbulence were extracted from a reference run without simulated turbulence from the same flight. When analyzing the data, it was found that this discrepancy between the simulated and the extracted turbulence is higher for higher levels of basic turbulence.

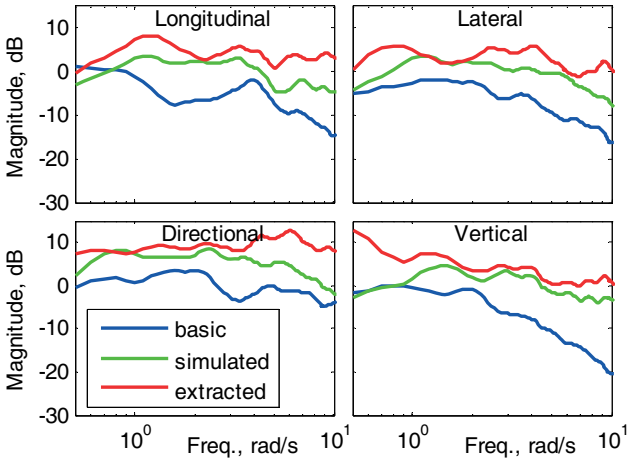

FIG 18. Comparison of simulated, extracted and basic turbulence

7.3. Structural Loads

Another way to validate the turbulence modeling process using control equivalent turbulence input models is the comparison of strain gauge measurements from flights with real and simulated turbulence. Strain gauges that measure the pitch and yaw bending moments of the tail boom are used to monitor structural loads during FHS experiments. Power spectral densities were determined from the measured bending moments for different flights with and without turbulence.

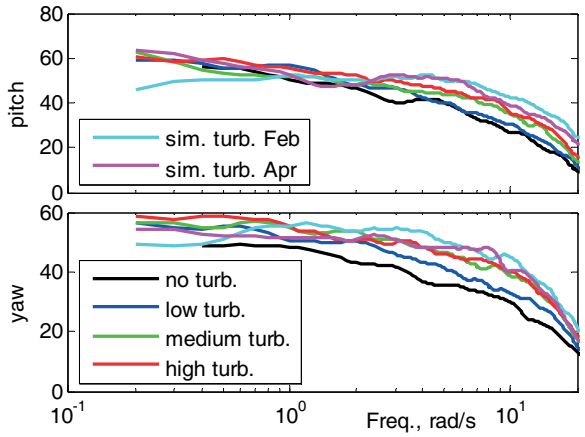

FIG 19. Structural loads from real and simulated turbulence flights

FIG 19 shows the PSDs for tests with the preliminary and the refined models in comparison to the results for the different turbulence levels from the data gathering flights

(averaged over each group of runs). Low pass filtered data was used for all cases. It can be seen, that the simulated turbulence with the refined models shows an improvement compared to the preliminary model and matches well with the real turbulence data. The overall increase of the loads due to turbulence effects can be seen when comparing to the reference case of no turbulence.

7.4. Handling Qualities Aspects

The turbulence model evaluation tests were performed with the same pilots that had performed the data gathering flights. During the flight tests at master gain value of 0.8 to 1.0 they stated to have the same workload compared to the data gathering flight and that they recognize the same aircraft response.

First handling qualities (HQ) evaluations performing the ADS-33 hover task in front of a hover board showed a decrease in performance from desired to adequate, and a change in Cooper Harper rating from 4 to 6. This compares well with findings by AFDD for handling qualities tasks performed in calm air and under turbulent conditions [15] who also noted a degradation of HQ ratings by 2 points for tests with turbulence.

During a visit of Empire Test Pilot School the turbulence model implementation was demonstrated to tutorial pilots. Performing the ADS-33 hover task, the turbulence was rated as quite realistic, leading to a significantly raised workload to stabilize the helicopter. 'It feels like hovering on a real gusty day with a bad aircraft'. (The FHS was flown without any stabilization.)

8. SUMMARY AND CONCLUSIONS

The development and initial flight testing of a Control Equivalent Turbulence Input (CETI) model for the EC 135 helicopter has been presented. The CETI model is comprised of four white noise driven filters, one for each control input. This formulation is very attractive for control system optimization and handling qualities evaluations because it is easy to implement for both ground based and in-flight simulations and has been derived from flight test data.

Regarding the analysis of the EC 135 data, the following conclusions can be drawn

- The effects of atmospheric turbulence on a hovering rotorcraft can be effectively modeled and simulated using the CETI method.
- High fidelity math-models that include higher-order effects are required for accurate extraction of control equivalent turbulence inputs for this type of turbulence modeling.
- The results shown demonstrate the effective application of system/parameter identification methods for different aspects of helicopter modeling.

Regarding the applicability of the derived CETI model to other helicopters, work is currently under way to develop a generalized CETI model that is scalable between conventional single rotor helicopters based on aircraft specific parameters such as rotor diameter, aircraft mass and inertias, etc.

9. REFERENCES

[1] R.E. McFarland, K. Duisenberg: "Simulation of Rotor Blade Element Turbulence", NASA Technical Memorandum 108862, Jan. 1995.

[2] Gaonkar, G.H.: "Review of Turbulence Modeling and Related Applications to Some Problems of Helicopter Flight Dynamics", Journal of the American Helicopter Society, Vol. 53, no. 1, Jan 2008, p. 87-107.

[3] Baillie, S. and Morgan, J., "An In-flight Investigation into the Relationships Among Control Sensitivity, Control Bandwidth and Disturbance Rejection Bandwidth Using a Variable Stability Helicopter," 15th European Rotorcraft Forum, Amsterdam, Netherlands, Sep. 1989.

[4] Labows, S., "UH-60 Black Hawk Disturbance Rejection Study for Hover/Low Speed Handling Qualities Criteria and Turbulence Modeling," M.S. Thesis, Naval Postgraduate School, Monterey, Calif., Mar. 2000.

[5] Lusardi, J., Tischler, M., Blanken, C., Labows, S., "Empirically Derived Helicopter Response Model and Control System Requirements for Flight in Turbulence," Journal of the American Helicopter Society, Vol. 49, no. 3, Jul. 2004, p. 340.

[6] Lusardi, J., Blanken, C., Tischler, M.: "Piloted Evaluation of a UH-60 Mixer equivalent Turbulence Simulation Model", AHS 59th Annual Forum, Phoenix, Arizona, May 6-8, 2003.

[7] J. J. Buchholz, W. von Gruenhagen: „Inversion Impossible?", DLR Institute Report IB 111 2003/34, Dec. 2003.

[8] Seher-Weiss, S., von Gruenhagen, W., "EC135 System Identification for Model Following Control and Turbulence Modeling," First CEAS European Air and Space Conference, Berlin, Germany, Sep. 2007, Paper No. CEAS-2007-275.

[9] Tischler M., Caufmann, M., "Frequency Response Method for Rotorcraft System Identification: Flight Applications to Bo 105 Coupled Rotor/Fuselage Dynamics", AHS Journal, Vol. 37, No. 4, 1992.

[10] Hamers, M., Lantzsch, R., Wolfram, J.: "First Control System Evaluation of the Research Helicopter FHS", 33rd European Rotorcraft Forum, Kazan, Russia, Sep. 11-13, 2007.

[11] Lantzsch, R., Hamers, M., Wolfram, J.: "Handling the Air Resonance Mode for Flight Control and Handling Qualities Evaluations on the DLR Research Helicopter FHS", Rotorcraft Handling Qualities Conference, The Foresight Centre, University of Liverpool, UK, 4-6 Nov. 2008.

[12] Ockier, C.: "The Art of Frequency Response Calculation", Institute Report DLR-IB 111 97/07, 1997.

[13] Lusardi, J., "Control Equivalent Turbulence Input Model for the UH-60 Helicopter", Dissertation, UC Davis, 2004.

[14] Seher-Weiss, S.: "User's Guide FITLAB – Parameter Estimation Using MATLAB – Version 2.0", Institute Report DLR IB-2007/27, 2007.

[15] Lusardi, J., von Gruenhagen, W. Seher-Weiss, S.: "Parametric Turbulence Modeling for Rotorcraft Applications- Approach, Flight Tests and Verification", Rotorcraft Handling Qualities Conference, The Foresight Centre, University of Liverpool, UK, 4-6 Nov. 2008.